Published for SISSA by Springer

Received: *September 14, 2022*
Accepted: *October 28, 2022*
Published: *November 14, 2022*

A predictive and testable unified theory of fermion masses, mixing and leptogenesis

Bowen Fu,[a] Stephen F. King,[a] Luca Marsili,[b] Silvia Pascoli,[b,c,d] Jessica Turner[e] and Ye-Ling Zhou[f,g]

[a] *School of Physics and Astronomy, University of Southampton, Southampton, SO17 1BJ, U.K.*
[b] *Dipartimento di Fisica e Astronomia, Università di Bologna, via Irnerio 46, 40126 Bologna, Italy*
[c] *INFN, Sezione di Bologna, viale Berti Pichat 6/2, 40127 Bologna, Italy*
[d] *CERN, Theoretical Physics Department, Geneva, Switzerland*
[e] *Institute for Particle Physics Phenomenology, Department of Physics, Durham University, Durham DH1 3LE, U.K.*
[f] *School of Fundamental Physics and Mathematical Sciences, Hangzhou Institute for Advanced Study, UCAS, Hangzhou, China*
[g] *International Centre for Theoretical Physics Asia-Pacific, Beijing/Hangzhou, China*

E-mail: b.fu@soton.ac.uk, s.f.king@soton.ac.uk, luca.marsili@studio.unibo.it, silvia.pascoli@unibo.it, jessica.turner@durham.ac.uk, zhouyeling@ucas.ac.cn

Abstract: We consider a minimal non-supersymmetric SO(10) Grand Unified Theory (GUT) model that can reproduce the observed fermionic masses and mixing parameters of the Standard Model. We calculate the scales of spontaneous symmetry breaking from the GUT to the Standard Model gauge group using two-loop renormalisation group equations. This procedure determines the proton decay rate and the scale of $\mathrm{U}(1)_{B-L}$ breaking, which generates cosmic strings and the right-handed neutrino mass scales. Consequently, the regions of parameter space where thermal leptogenesis is viable are identified and correlated with the fermion masses and mixing, the neutrinoless double beta decay rate, the proton decay rate, and the gravitational wave signal resulting from the network of cosmic strings. We demonstrate that this framework, which can explain the Standard Model fermion masses and mixing and the observed baryon asymmetry, will be highly constrained by the next

https://doi.org/10.1007/JHEP11(2022)072

JHEP11(2022)072

generation of gravitational wave detectors and neutrino oscillation experiments which will also constrain the proton lifetime.

Keywords: Grand Unification, Neutrino Mixing, Baryo-and Leptogenesis, Early Universe Particle Physics

ArXiv ePrint: 2209.00021

Contents

1 Introduction

Grand Unified Theories (GUTs) have long been an attractive framework for unifying the non-gravitational interactions. The minimal option, which can predict neutrino masses and mixing, uses the gauge group SO(10). Several well-studied symmetries can be embedded in SO(10), including SU(5) [1], flipped SU(5) $\times$ U(1) [2–5] and the Pati-Salam model $\mathrm{SU}(4)_c \times \mathrm{SU}(2)_L \times \mathrm{SU}(2)_R$ [6]. Thanks to this rich structure, there are many possible symmetry-breaking chains from SO(10) down to the Standard Model (SM) gauge group, G_{SM}, most of them via the Pati-Salam symmetry [7]. An appealing feature of an intermediate Pati-Salam symmetry in non-supersymmetric GUTs is that gauge unification can be achieved, and there is an intermediate $\mathrm{U}(1)_{B-L}$ subgroup which is spontaneously broken, generating right-handed neutrino masses. In addition to inducing light neutrino masses via the seesaw mechanism, the CP-violating and out-of-equilibrium decays of the right-handed neutrinos can produce the observed matter-antimatter asymmetry via thermal leptogenesis [8]. Moreover, the $\mathrm{U}(1)_{B-L}$ symmetry breaking can also generate cosmic strings in the early Universe, which can intercommute and emit gravitational radiation forming a stochastic gravitational wave (GW) background that future GW interferometers can test.

The connection between GUTs and gravitational waves has been studied in [9] where the simple breaking pattern $\mathrm{SO}(10) \to G_{\mathrm{SM}} \times \mathrm{U}(1)_{B-L} \to G_{\mathrm{SM}}$ was shown to be consistent with inflation, leptogenesis, and dark matter, while the $\mathrm{U}(1)_{B-L}$ symmetry breaking generates cosmic strings. The connection between high-scale thermal leptogenesis and GWs was also

JHEP11(2022)072

pointed in [10] where it was assumed that the $\mathrm{U}(1)_{B-L}$ breaking scale is the same as the seesaw and leptogenesis scales. In ref. [11], we highlighted the complementarity between proton decay and gravitational wave signals from cosmic strings as a powerful method of probing GUTs. Subsequently, in ref. [12], we studied all possible non-supersymmetric SO(10) symmetry-breaking chains. We performed a comprehensive renormalisation group (RG) analysis to find the correlations between the proton decay rate and the GW signal. We also identified which chains survived the current non-observation of both proton decay and GWs and could be tested by future neutrino and GW experiments.

In this paper, we go beyond these works by providing a detailed study on a specific SO(10) breaking chain that provides unification and predicts a proton decay width via the channel $p \to \pi^0 e^+$, consistent with the experimental bound of the Super-Kamiokande (Super-K) [13] and can be fully tested by future proton decay searches of Hyper-K [12]. Further, this breaking chain generates cosmic strings at the lowest intermediate scale, $M_1 \sim 10^{13}\,\mathrm{GeV}$. A GW background generated by such a string network is just around the corner and may be even already hinted at by recent observations in PTA experiments, including NANOGrav [14], PPTA [15], EPTA [16] and IPTA [17]. We determine the minimal necessary particle content to induce the pattern of breaking and perform an RG analysis and numerical fit of our model to SM data to postdict the fermion masses and mixing, including the mass scales of the right-handed neutrinos. As this procedure determines the scales of symmetry breaking of our model and the masses of the right-handed neutrinos, the matter-antimatter asymmetry associated with thermal leptogenesis is predicted. We then show that successful leptogenesis can occur in the regions of the model parameter space consistent with SM fermion masses and mixing and can be correlated with a GW signal and proton decay. Compared with [10], such an approach allows us to go beyond generic considerations and instead to quantitatively account for the hierarchy between the leptogenesis and see-saw scales, as well as with the $\mathrm{U}(1)_{B-L}$ breaking scale, thanks to the constraints imposed by reproducing the low energy data. The latter scale is of particular interest since pulsar timing arrays such as PPTA [18] and NANOGrav [19] are sensitive to the predicted GW signals while future large-scale neutrino experiment, Hyper-Kamiokande (Hyper-K) [20], will be able to probe the predicted proton decay rate of this model. The correlation between these two observables will be a crucial test of our GUT model, and such methodology can be applied to other GUT models, presenting a new avenue to try to unveil the physics at very high scales.

This paper is organised as follows: in section 2, we discuss the GUT symmetry breaking pattern and the particle content of our model, including fermionic and Higgs representations of the GUT and our RG running procedure. In section 3, we discuss how we relate our model to the quark lepton data, our fitting procedure and the ensuing results. In section 4, we discuss the basics of non-resonant thermal leptogenesis and how we determine the baryon asymmetry produced from the successful points in the model parameter space and in section 5, we demonstrate that the regions of the model parameter space that yield successful leptogenesis and fermionic masses and mixing will be associated with a GW signal. Finally, we summarise and discuss in section 6. As a case study, we consider a benchmark point (referred to as BP1 throughout) and discuss how it satisfies all these experimental constraints in each section.

JHEP11(2022)072

2 The framework

We focus on a breaking chain (classified as chain III4 of type (c) in ref. [12]) that is of particular interest as it is currently allowed and predicts a proton decay rate testable by Hyper-K. We discuss the breaking chain's matter content and gauge unification in this section.

2.1 Symmetry breaking of SO(10)

We study the following breaking chain with three intermediate symmetries (G_3, G_2, and G_1):

$$\begin{aligned}
&\mathrm{SO}(10)\\
&\mathbf{54}\big\downarrow \text{ broken at } M_X\\
&G_3 \equiv \mathrm{SU}(4)\times\mathrm{SU}(2)_L\times\mathrm{SU}(2)_R\times Z_2^C\\
&\mathbf{210}\big\downarrow \text{ broken at } M_3\\
&G_2 \equiv \mathrm{SU}(3)_c\times\mathrm{SU}(2)_L\times\mathrm{SU}(2)_R\times\mathrm{U}(1)_X\times Z_2^C\\
&\mathbf{45}\big\downarrow \text{ broken at } M_2\\
&G_1 \equiv \mathrm{SU}(3)_c\times\mathrm{SU}(2)_L\times\mathrm{SU}(2)_R\times\mathrm{U}(1)_X\\
&\overline{\mathbf{126}}\big\downarrow \text{ broken at } M_1\\
&G_{\mathrm{SM}} \equiv \mathrm{SU}(3)_c\times\mathrm{SU}(2)_L\times\mathrm{U}(1)_Y\,.
\end{aligned}\tag{2.1}$$

The boldface number beside the arrow indicates the Higgs representation of SO(10), triggering the symmetry breaking. In this work, we follow the same convention as ref. [12] where the GUT symmetry breaking scale is denoted as M_X and the mass scale of the subsequent breaking of the group G_I (for $I = 1, 2, 3$) is denoted as M_I.[1] All particles, except the gauge fields of the model, are listed in table 1. We note that Z_2^C refers to the parity symmetry between left and right conjugation ($L \leftrightarrow R^c$, where c indicates charge conjugation) and that $\mathrm{U}(1)_X$ is identical to the $\mathrm{U}(1)_{B-L}$ symmetry with the charge correlated via $X = \sqrt{\frac{3}{2}}(\frac{B-L}{2})$. The correlations between U(1) charges are given by $Y = \sqrt{\frac{3}{5}}\left(I_{3R} + \frac{B-L}{2}\right)$, where I_{3R} is the isospin in $\mathrm{SU}(2)_R$.

To achieve each step of symmetry breaking, i.e., $\mathrm{SO}(10) \to G_3 \to G_2 \to G_1$, we include three Higgs multiplets, **54**, **210**, and **45** of SO(10), respectively. These Higgs fields spontaneously break the GUT symmetry as follows:

- **54** contains a parity-even singlet $(\mathbf{1},\mathbf{1},\mathbf{1})$ of $G_3 \equiv \mathrm{SU}(4)_c\times\mathrm{SU}(2)_L\times\mathrm{SU}(2)_R$ where each entry in the bracket $(\mathbf{r_1},\mathbf{r_2},\cdots)$ refers to the field representation transforming in the group $G \equiv H_1 \times H_2 \times \cdots$. Once $(\mathbf{1},\mathbf{1},\mathbf{1})$ gains a non-trivial vacuum expectation value (VEV) at scale M_X, SO(10) is spontaneously broken to G_3.
- In G_3, **210** can be decomposed to $(\mathbf{15},\mathbf{1},\mathbf{1})_1$ of G_3, which is further decomposed into a parity-even and trivial singlet $(\mathbf{1},\mathbf{1},\mathbf{1},0)_1$ of $\mathrm{SU}(3)_c\times\mathrm{SU}(2)_L\times\mathrm{SU}(2)_R\times\mathrm{U}(1)_X$,

[1] However, we change the notation of the running energy scale to from μ to Q as the string tension is often denoted as μ.

JHEP11(2022)072

	Multiplet	Role in the model
Fermions	**16**	Contains all SM fermions and RH neutrinos
Higgses	**10**	Generates fermion masses
	45	Triggers intermediate symmetry breaking
	54	Triggers GUT symmetry breaking
	120	Generates fermion masses
	$\overline{\mathbf{126}}$	Generates fermion masses & intermediate symmetry breaking
	210	Triggers intermediate symmetry breaking

Table 1. The SO(10) representations of the fermion and Higgs particles of our SO(10) GUT model and their roles.

SO(10)	**54**	**210**	**45**	$\overline{\mathbf{126}}$
G_3	$(\mathbf{1},\mathbf{1},\mathbf{1})$	$(\mathbf{15},\mathbf{1},\mathbf{1})_1$	$(\mathbf{15},\mathbf{1},\mathbf{1})_2$	$(\mathbf{10},\mathbf{1},\mathbf{3})+(\overline{\mathbf{10}},\mathbf{3},\mathbf{1})$
G_2	–	$(\mathbf{1},\mathbf{1},\mathbf{1},0)_1$	$(\mathbf{1},\mathbf{1},\mathbf{1},0)_2$	$(\mathbf{1},\mathbf{1},\mathbf{3},-1)+(\mathbf{1},\mathbf{3},\mathbf{1},1)$
G_1	–	–	$(\mathbf{1},\mathbf{1},\mathbf{1},0)_2$	$(\mathbf{1},\mathbf{1},\mathbf{3},-1)$
G_{SM}	–	–	–	$(\mathbf{1},\mathbf{1},0)_S$

Table 2. Decomposition of the Higgses which induce spontaneous symmetry breaking at each step of the breaking chain. Each Higgs (from left to right) is eventually decomposed to a singlet whose non-vanishing VEV preserves the symmetry G_I (for $I = 3, 2, 1, \mathrm{SM}$) in the same row but breaks larger symmetries. The subscript distinguishes different fields of the same representation.

where the last entry in the bracket is the field charge in the U(1) symmetry and the subscript is used to distinguish from another field with the same representation discussed below. The VEV of this singlet breaks G_3 to G_2 at scale M_3.

- The breaking of G_2 to G_1 is realised via a **45** of SO(10), which decomposed into $(\mathbf{15},\mathbf{1},\mathbf{1})_2$ of G_3 and a further $(\mathbf{1},\mathbf{1},\mathbf{1},0)_2$ of G_2 and G_1. This singlet is parity-odd, and its VEV induces the breaking of $G_2 \to G_1$ at scale M_2.
- Finally, the breaking of $G_1 \to G_{\mathrm{SM}}$ at scale M_1 is provided by $\overline{\mathbf{126}}$, which is decomposed into a triplet $(\mathbf{1},\mathbf{1},\mathbf{3},-1)$ of $\mathrm{SU}(3)_c \times \mathrm{SU}(2)_L \times \mathrm{SU}(2)_R \times \mathrm{U}(1)_X$ and to a further singlet, $(\mathbf{1},\mathbf{1},0)$, of G_{SM}. This singlet field, denoted as ϕ_S, provides mass to the three right-handed neutrinos.

We summarise the decomposition of Higgses, which triggers the breaking of SO(10) and intermediate symmetries, in table 2.

2.2 Matter field decomposition and fermion masses

In order to assess if our model can predict the measured fermionic masses and mixing, it is important to understand the matter content of the breaking chain. Fermions are arranged as a **16** of SO(10) and follow the decomposition given in table 3 where L (R) denote the

JHEP11(2022)072

SO(10)	**16**
G_3	$(\mathbf{4},\mathbf{2},\mathbf{1})_L + (\overline{\mathbf{4}},\mathbf{1},\mathbf{2})_{R^c}$
G_2	$(\mathbf{3},\mathbf{2},\mathbf{1},1/6)_{Q_L} + (\overline{\mathbf{3}},\mathbf{1},\mathbf{2},-1/6)_{Q_R^c}$ $+(\mathbf{1},\mathbf{2},\mathbf{1},-1/2)_{l_L} + (\mathbf{1},\mathbf{1},\mathbf{2},1/2)_{l_R^c}$
G_1	$(\mathbf{3},\mathbf{2},\mathbf{1},1/6)_{Q_L} + (\overline{\mathbf{3}},\mathbf{1},\mathbf{2},-1/6)_{Q_R^c}$ $+(\mathbf{1},\mathbf{2},\mathbf{1},-1/2)_{l_L} + (\mathbf{1},\mathbf{1},\mathbf{2},1/2)_{l_R^c}$
$G_{\rm SM}$	$(\mathbf{3},\mathbf{2},1/6)_{Q_L} + (\overline{\mathbf{3}},\mathbf{1},-2/3)_{u_R^c} + (\overline{\mathbf{3}},\mathbf{1},1/3)_{d_R^c}$ $+(\mathbf{1},\mathbf{2},-1/2)_{l_L} + (\mathbf{1},\mathbf{1},0)_{\nu_R^c} + (\mathbf{1},\mathbf{1},1)_{e_R^c}$

Table 3. Decomposition of the matter multiplet **16** in each step of the breaking chain.

left-handed (right-handed) fermions of G_3 which contains the SM left-handed (right-handed) fermions where $Q_{L(R)}$ and $\ell_{L(R)}$ are the quark and leptonic $\mathrm{SU}(2)_{L(R)}$ doublets, respectively, and u_R, d_R, e_R, and ν_R are the quark and lepton $\mathrm{SU}(2)_L$ singlets, respectively.

Three Higgs multiplets, **10**, $\overline{\mathbf{126}}$ and **120**, are required to generate the Standard Model fermion masses. Compared to ref. [12], where we considered a minimal survival hypothesis [21], we include one additional Higgs (**120**) which is required to generate all fermion mass spectra, mixing angles, and CP-violating phases in the quark and lepton sectors. Here, $\overline{\mathbf{126}}$ is the same Higgs used in the breaking $G_1 \to G_{\rm SM}$. For this breaking chain, we list decompositions of Higgs, which are responsible for mass generation in table 2.

Applying this decomposition, we have two $(\mathbf{1},\mathbf{2},\mathbf{2})$ and two $(\mathbf{15},\mathbf{2},\mathbf{2})$ multiplets of G_3 after the SO(10) breaking. These multiplets are composed of four bi-doublets, $(\mathbf{1},\mathbf{2},\mathbf{2},0)$, of G_2 and G_1. After $\mathrm{SU}(2)_R$ is broken below M_1, each bi-doublet contains two electroweak doublets $(\mathbf{1},\mathbf{2},\mp 1/2)$, and eventually, we arrive at the eight electroweak doublets of the model which we denote as $h_i = \{\tilde{h}^u_{\mathbf{10}}, \tilde{h}^u_{\overline{\mathbf{126}}}, \tilde{h}^u_{\mathbf{120}}, \tilde{h}^{u'}_{\mathbf{120}}, h^d_{\mathbf{10}}, h^d_{\overline{\mathbf{126}}}, h^d_{\mathbf{120}}, h^{d'}_{\mathbf{120}}\}$, where $\tilde{h}^u_{\mathbf{10}} = i\sigma_2 (h^u_{\mathbf{10}})^*$. These field decompositions introduce particles beyond the SM spectrum and may contribute to the renormalisation group running behaviour of the gauge coefficients. However, we reduce their redundancy in the following way: for scale Q which varies in the range $M_X > Q > M_3$, where G_3 is preserved, the two decomposed $(\mathbf{1},\mathbf{2},\mathbf{2})$'s can mix and we assume that the heavy one gains a mass $\sim M_X$ and thus decouples at scales below M_X. The same assumption applies to the other two $(\mathbf{1},\mathbf{2},\mathbf{2})$'s. Using these assumptions, we have two bi-doublets $(\mathbf{1},\mathbf{2},\mathbf{2},0)$ at the scale $M_3 > Q > M_2$ and $M_2 > Q > M_1$, where G_2 and G_1 are preserved, respectively. We retain them as the physically relevant degrees of freedom in this range of scales, following the logic of ref. [12]. Four electroweak doublets remain at energies below M_1 but above the electroweak scale. Naively, one can assume all massive states are sufficiently heavy that they decouple at scale M_1, except for the lightest electroweak doublet, which is the SM Higgs and should be massless before electroweak symmetry breaking. Without loss of generality, we can write these Higgses as superpositions of mass eigenstates, $\hat{h}_i = \sum_j V_{ij} h_j$, with $h_{\rm SM} \equiv \hat{h}_1$, where V is a unitary matrix and

SO(10)	$\mathbf{10}$	$\overline{\mathbf{126}}$	$\mathbf{120}$
G_3	$(\mathbf{1},\mathbf{2},\mathbf{2})_1$	$(\mathbf{15},\mathbf{2},\mathbf{2})_1$ $+(\mathbf{10},\mathbf{1},\mathbf{3})+(\overline{\mathbf{10}},\mathbf{3},\mathbf{1})$	$(\mathbf{1},\mathbf{2},\mathbf{2})_2+(\mathbf{15},\mathbf{2},\mathbf{2})_2$
G_2	$(\mathbf{1},\mathbf{2},\mathbf{2},0)_1$	$(\mathbf{1},\mathbf{2},\mathbf{2},0)_2$ $+(\mathbf{1},\mathbf{1},\mathbf{3},-1)+(\mathbf{1},\mathbf{3},\mathbf{1},1)$	$(\mathbf{1},\mathbf{2},\mathbf{2},0)_{3,4}$
G_1	$(\mathbf{1},\mathbf{2},\mathbf{2},0)_1$	$(\mathbf{1},\mathbf{2},\mathbf{2},0)_2$ $+(\mathbf{1},\mathbf{1},\mathbf{3},-1)$	$(\mathbf{1},\mathbf{2},\mathbf{2},0)_{3,4}$
$G_{\rm SM}$	$(\mathbf{1},\mathbf{2},-1/2)_{h^u_{\mathbf{10}}}$ $+(\mathbf{1},\mathbf{2},+1/2)_{h^d_{\mathbf{10}}}$	$(\mathbf{1},\mathbf{2},-1/2)_{h^u_{\overline{\mathbf{126}}}}$ $+(\mathbf{1},\mathbf{2},+1/2)_{h^d_{\overline{\mathbf{126}}}}$ $+(\mathbf{1},\mathbf{1},0)_S$	$(\mathbf{1},\mathbf{2},-1/2)_{h^u_{\mathbf{120}},h^{u'}_{\mathbf{120}}}$ $+(\mathbf{1},\mathbf{2},+1/2)_{h^d_{\mathbf{120}},h^{d'}_{\mathbf{120}}}$

Table 4. Decomposition of Higgses responsible for the fermion mass generation. $\overline{\mathbf{126}}$ is the same Higgs as shown in table 2 and it is responsible for both the breaking $G_1 \to G_{\rm SM}$ and right-handed neutrino mass generation. $(\mathbf{1},\mathbf{1},0)_S$ is the same singlet given in table 2.

the heavy doublets that decouple at M_X have also been taken into account. With this treatment, all physical degrees of freedom present at the relevant scale are the same as those of chain III4 in ref. [12]. For the second Higgs multiplet, $\overline{\mathbf{126}}$, we retain another decomposed representation $(\mathbf{10},\mathbf{3},\mathbf{1})$ of G_1, which contains a SU(2)$_L$ triplet, $(\mathbf{1},\mathbf{1},\mathbf{3},-1)$, of G_2 and G_1 which contains the singlet $S \sim (\mathbf{1},\mathbf{1},0)$ of $G_{\rm SM}$ that is important not only in its role in symmetry breaking, but also in the generation of neutrino masses. $(\overline{\mathbf{10}},\mathbf{3},\mathbf{1})$ is retained due to the requirement of left-right parity symmetry, Z_2^C, and it is decomposed to a $(\mathbf{1},\mathbf{3},\mathbf{1},1)$ of G_2. After G_2 breaking, i.e., the breaking of the left-right parity symmetry, we assume that this particle decouples.

In the Yukawa sector, couplings above the GUT scale are given by

$$Y^*_{\mathbf{10}}\,\mathbf{16}\cdot\mathbf{16}\cdot\mathbf{10}+Y^*_{\overline{\mathbf{126}}}\,\mathbf{16}\cdot\mathbf{16}\cdot\overline{\mathbf{126}}+Y^*_{\mathbf{120}}\,\mathbf{16}\cdot\mathbf{16}\cdot\mathbf{120}+\text{h.c.}\,, \tag{2.2}$$

where the asterisk denotes complex conjugation. Considering the flavour indices, $Y_{\mathbf{10}}$ and $Y_{\overline{\mathbf{126}}}$ are in general complex 3×3 symmetric matrices and $Y_{\mathbf{120}}$ is an antisymmetric matrix. In the non-SUSY case, two further couplings $\mathbf{16}\cdot\mathbf{16}\cdot\mathbf{10}^*$ and $\mathbf{16}\cdot\mathbf{16}\cdot\mathbf{120}^*$ are allowed by the gauge symmetry; however, we forbid them by imposing an additional Peccei-Quinn U(1) symmetry [22] as described in [23–25]. After the final symmetry is broken to $G_{\rm SM}$, the above Yukawa terms generate the following SM fermion mass terms in the left-right convention:

$$\begin{aligned}&Y_{\mathbf{10}}\left[(\overline{Q}u_R+\overline{L}\nu_R)\,h^u_{\mathbf{10}}+(\overline{Q}d_R+\overline{L}e_R)\,h^d_{\mathbf{10}}\right]+\frac{1}{\sqrt{3}}Y_{\overline{\mathbf{126}}}\left[(\overline{Q}u_R-3\overline{L}\nu_R)\,h^u_{\overline{\mathbf{126}}}+(\overline{Q}d_R-3\overline{L}e_R)\,h^d_{\overline{\mathbf{126}}}\right]\\&+Y_{\mathbf{120}}\left[(\overline{Q}u_R+\overline{L}\nu_R)\,h^u_{\mathbf{120}}+(\overline{Q}d_R+\overline{L}e_R)\,h^d_{\mathbf{120}}+\frac{1}{\sqrt{3}}(\overline{Q}u_R-3\overline{L}\nu_R)\,h^{u'}_{\mathbf{120}}+(\overline{Q}d_R-3\overline{L}e_R)h^{d'}_{\mathbf{120}}\right]+\text{h.c.}\end{aligned} \tag{2.3}$$

Rotating the Higgs fields to their mass basis, we derive Yukawa couplings to the SM Higgs as

$$Y_u\overline{Q}\,\tilde{h}_{\rm SM}\,u_R+Y_d\overline{Q}\,h_{\rm SM}\,d_R+Y_\nu\overline{L}\,\tilde{h}_{\rm SM}\,\nu_R+Y_e\overline{L}\,h_{\rm SM}\,e_R+\text{h.c.}\,, \tag{2.4}$$

JHEP11(2022)072

where

$$\begin{aligned}
Y_u &= Y_{\mathbf{10}} V_{11}^* + \frac{1}{\sqrt{3}} Y_{\overline{\mathbf{126}}} V_{12}^* + Y_{\mathbf{120}} \left(V_{13}^* + \frac{1}{\sqrt{3}} V_{14}^* \right) , \\
Y_d &= Y_{\mathbf{10}} V_{15} + \frac{1}{\sqrt{3}} Y_{\overline{\mathbf{126}}} V_{16} + Y_{\mathbf{120}} \left(V_{17} + \frac{1}{\sqrt{3}} V_{18} \right) , \\
Y_\nu &= Y_{\mathbf{10}} V_{11}^* - \sqrt{3} Y_{\overline{\mathbf{126}}} V_{12}^* + Y_{\mathbf{120}} \left(V_{13}^* - \sqrt{3} V_{14}^* \right) , \\
Y_e &= Y_{\mathbf{10}} V_{15} - \sqrt{3} Y_{\overline{\mathbf{126}}} V_{16} + Y_{\mathbf{120}} \left(V_{17} - \sqrt{3} V_{18} \right) .
\end{aligned} \tag{2.5}$$

A Majorana mass term for the right-handed neutrinos is generated from the second term of eq. (2.2):

$$Y_{\overline{\mathbf{126}}} \overline{\nu}_R \, \phi_S \, \nu_R^c + \text{h.c.} , \tag{2.6}$$

once ϕ_S acquires a VEV, v_S, which controls the scale of the masses:

$$M_{\nu_R} = Y_{\overline{\mathbf{126}}} \, v_S \, . \tag{2.7}$$

After the right-handed neutrinos decouple and electroweak symmetry is broken, the light neutrinos acquire their mass via the Type-I seesaw mechanism [26–29]:

$$M_\nu = - Y_\nu M_{\nu_R}^{-1} Y_\nu^T v_{\text{SM}}^2 , \tag{2.8}$$

where the SM Higgs VEV is $v_{\text{SM}} = 175\,\text{GeV}$. We emphasise that the electroweak singlet, ϕ_S, is essential for the symmetry breaking $G_1 \to G_{\text{SM}}$ and thus, its VEV determines the scale of M_1 and the right-handed neutrino masses. As required by perturbativity, $Y_{\overline{\mathbf{126}}} \lesssim \mathcal{O}(1)$, the mass of the heaviest right-handed neutrino, M_{N_3}, should be not heavier than the lowest intermediate scale, M_1. On the other hand, neutrino oscillation experiments have given relatively precise measurements of light neutrino masses and mixing angles. These data restrict the right-handed neutrino mass spectrum via the seesaw formula, and a realistic GUT model should survive all such constraints.

2.3 Gauge unification

Given an arbitrary gauge symmetry G, which can be expressed as a product of simple Lie groups, $G = H_1 \times \cdots \times H_n$, the two-loop renormalisation group running equation for group H_i, for $i = 1, 2, \cdots$, is given by

$$Q \frac{d\alpha_i}{dQ} = \beta_i(\alpha_i) , \tag{2.9}$$

where $\alpha_i = g_i^2/(4\pi)$ and the β function is determined by the particle content of the theory:

$$\beta_i = -\frac{1}{2\pi} \alpha_i^2 \left(b_i + \frac{1}{4\pi} \sum_j b_{ij} \alpha_j \right) . \tag{2.10}$$

Here, $i \in [1, \cdots, n]$ for H_n, g_i is the gauge coefficient of H_i, and b_i and b_{ij} refer to the normalised coefficients of one- and two-loop contributions, respectively. In the following, we

JHEP11(2022)072

neglect the Yukawa contribution to the RG running equations as it gives a subdominant contribution. Given two scales Q_0 and Q, if the conditions $Q_0 < Q$ and $b_j \alpha_j(Q_0) \log(Q/Q_0) < 1$ are both satisfied then an analytical solution for these equations can be obtained [30]:

$$\alpha_i^{-1}(Q) = \alpha_i^{-1}(Q_0) - \frac{b_i}{2\pi} \log \frac{Q}{Q_0} + \sum_j \frac{b_{ij}}{4\pi b_i} \log \left(1 - \frac{b_j}{2\pi} \alpha_j(Q_0) \log \frac{Q}{Q_0}\right) . \tag{2.11}$$

In the case that both H_i and H_j are non-abelian groups, the coefficients b_i and b_{ij} are

$$\begin{aligned} b_i &= -\frac{11}{3} C_2(H_i) + \frac{2}{3} \sum_F T(\psi_i) + \frac{1}{3} \sum_S T(\phi_i) , \\ b_{ij} &= -\frac{34}{3} [C_2(H_i)]^2 \delta_{ij} + \sum_F T(\psi_i) \left[2C_2(\psi_j) + \frac{10}{3} C_2(H_i) \delta_{ij}\right] \\ &\quad + \sum_S T(\phi_i) \left[4C_2(\phi_j) + \frac{2}{3} C_2(H_i) \delta_{ij}\right] , \end{aligned} \tag{2.12}$$

where the ψ and ϕ indices sum over the fermions and complex scalar multiplets, respectively, and ψ_i and ϕ_i are their representations in the group H_i, respectively. $C_2(R_i)$ (for $R_i = \psi_i, \phi_i$) denotes the quadratic Casimir of the representation R_i in group H_i and $C_2(H_i)$ is the quadratic Casimir of the adjoint presentation of the group H_i.

In particular, for SU(N), $C_2(\mathrm{SU}(N)) = N$ and the quadratic Casimir of the fundamental irrep $\mathbf{N}$ of SU(N) is given by $C_2(\mathbf{N}) = (N^2 - 1)/2N$; for SO(10), $C_2(\mathrm{SO}(10)) = 8$, and the quadratic Casimir of the fundamental irrep **10** of SO(10) is given by $C_2(\mathbf{10}) = 9/2$. The spinor representation of SO(10), **16**, has $C_2(\mathbf{16}) = 45/4$. $T(R_i)$ is the Dynkin index of representation R_i of group H_i. For SU(N), $T(R_i) = C_2(R_i) d(R_i)/(N^2 - 1)$ where $d(R_i)$ is the dimension of R_i. If one of H_j is a U(1) symmetry, the coefficient b_{ij} is obtained by replacing $C_2(R_j)$ and $T(R_j)$ with the charge square $[Q_j(R)]^2$ of the field multiplet R in $\mathrm{U}(1)_j$. For the Abelian symmetry, $C_2(\mathrm{U}(1)) = 0$.

Explicit values of b_i and b_{ij} depend on the degree of freedoms introduced by the gauge, matter and Higgs fields. The gauge fields are directly determined by the gauge symmetry in the breaking chain. In regards to the matter fields, we assume they are the minimal extension which includes all the SM fermions, i.e., minimally a **16** of SO(10) as in table 3. The most significant uncertainty contributing to RG running comes from the Higgs sector as one has to account for all the Higgses used to generate fermion masses and the GUT and intermediate symmetry breaking. Given the decomposition of Higgs fields in table 2 and the discussion in section 2.2, the Higgs fields included in each step of the RG running are:

- For $G_1 \to G_{\mathrm{SM}}$, we include only the SM Higgs. Although we arrive at a series of electroweak doublets after field decomposition, we assume that all degrees of freedom except the SM Higgs are sufficiently heavy that they are integrated out by this breaking step and thus have a negligible effect on the RG running.

- For $G_2 \to G_1$, we include three Higgses in the running, two $(\mathbf{1}, \mathbf{2}, \mathbf{2}, 0)$'s and one $(\mathbf{1}, \mathbf{1}, \mathbf{3}, -1)$ of G_1. The former includes the SM Higgs, and the latter includes the gauge singlet ϕ_S of G_{SM} which is used to achieve the breaking of $G_1 \to G_{\mathrm{SM}}$ and right-handed neutrino masses.

- For $G_3 \to G_2$, we include two $(\mathbf{1}, \mathbf{2}, \mathbf{2}, 0)$'s, $(\mathbf{1}, \mathbf{1}, \mathbf{3}, -1)$, $(\mathbf{1}, \mathbf{3}, \mathbf{1}, 1)$, and $(\mathbf{1}, \mathbf{1}, \mathbf{1}, 0)_2$ in the RG running. Two further Higgses are included compared to the above item as $(\mathbf{1}, \mathbf{3}, \mathbf{1}, 1)$ is required for the matter parity symmetry Z_2^C and $(\mathbf{1}, \mathbf{1}, \mathbf{1}, 0)_2$ is used to break Z_2^C, $G_2 \to G_1$.
- For SO(10) $\to G_3$, we include $(\mathbf{1}, \mathbf{2}, \mathbf{2})$, $(\mathbf{15}, \mathbf{2}, \mathbf{2})$, $(\mathbf{10}, \mathbf{1}, \mathbf{3})$, $(\overline{\mathbf{10}}, \mathbf{3}, \mathbf{1})$ and two $(\mathbf{15}, \mathbf{1}, \mathbf{1})$'s in the RG running. The former two are required to obtain the two $(\mathbf{1}, \mathbf{2}, \mathbf{2}, 0)$'s above. $(\mathbf{10}, \mathbf{1}, \mathbf{3})$ and $(\overline{\mathbf{10}}, \mathbf{3}, \mathbf{1})$ are required for $(\mathbf{1}, \mathbf{1}, \mathbf{3}, -1)$ and $(\mathbf{1}, \mathbf{3}, \mathbf{1}, 1)$. One $(\mathbf{15}, \mathbf{1}, \mathbf{1})$, decomposed from $\mathbf{45}$ is for $(\mathbf{1}, \mathbf{1}, \mathbf{1}, 0)_2$, and the other, decomposed from 210, includes the singlet $(\mathbf{1}, \mathbf{1}, \mathbf{1}, 0)_1$ to achieve the breaking $G_3 \to G_2$.

By including the above particle content in the RG running, we obtain the coefficients b_i and b_{ij} at the two-loop level, which we list in table 5 and are the same as in the chain III4 of ref. [12]. Although we include one more Higgs multiplet $\mathbf{120}$, the contribution of induced new particles can be ignored, as explained in the previous subsection, by assuming heavy mass eigenstates heavier than the breaking scale, M_X [31]. In order to keep the treatment of the RG running economical, the scalar multiplets which are unnecessary for the breaking chain are assumed to be as massive as the SO(10) breaking scale M_X. Therefore, these scalars will not affect the RG running or provide threshold corrections.

During the symmetry breaking at an intermediate scale (M_3, M_2 or M_1), gauge couplings of the larger symmetry and those of the residual symmetry after spontaneous symmetry breaking (SSB) must satisfy matching conditions. Here we list one-loop matching conditions that appear in the GUT breaking chains. For a simple Lie group H_{i+1} broken to subgroup H_i at the scale $Q = M_I$, the one-loop matching condition is given by [32]

$$H_{i+1} \to H_i \; : \quad \alpha^{-1}_{H_{i+1}}(M_I) - \frac{1}{12\pi} C_2(H_{i+1}) = \alpha^{-1}_{H_i}(M_I) - \frac{1}{12\pi} C_2(H_i)\,. \tag{2.13}$$

For $G_1 \to G_{\rm SM}$, we encounter the breaking, $\mathrm{SU}(2)_R \times \mathrm{U}(1)_X \to \mathrm{U}(1)_Y$, which has the matching condition [33]:

$$\mathrm{SU}(2)_R \times \mathrm{U}(1)_X \to \mathrm{U}(1)_Y \; : \quad \frac{3}{5}\Big(\alpha^{-1}_{2R}(M_I) - \frac{1}{6\pi}\Big) + \frac{2}{5}\alpha^{-1}_{1X}(M_I) = \alpha^{-1}_{1Y}(M_1)\,. \tag{2.14}$$

Applying the matching conditions of the above two equations, all gauge couplings of the subgroups unify into a single gauge coupling, $\alpha_X \equiv g_X^2/4\pi$, of SO(10) at the GUT scale, M_X. This condition restricts both the GUT and intermediate scales for each breaking chain. We denote the mass of the heavy gauge boson masses associated with SO(10) breaking as M_X and M_3, M_2 and M_1 are associated to the breaking of G_3, G_2 and G_1, respectively. Correlations among M_1, M_2, M_3 and M_X are determined numerically using the following procedure for the breaking chain $\mathrm{SO}(10) \to G_3 \to G_2 \to G_1 \to G_{\rm SM}$ where the two-loop RG running evolution is performed in reverse, $G_{\rm SM} \to G_1 \to G_2 \to G_3 \to \mathrm{SO}(10)$:

1. Begin the evaluation from the scale M_Z with the SM gauge couplings $\alpha_3 = 0.1184$, $\alpha_2 = 0.033819$ and $\alpha_1 = 0.010168$ [34]. Evolve these couplings using the RGE of the SM to scale M_1, where G_1 is recovered. Apply the matching conditions for the SM gauge couplings and the G_1 gauge couplings to obtain the values of couplings in the intermediate symmetry group.

JHEP11(2022)072

SO(10)	broken at $Q = M_X$
$\downarrow$	$\{b_i\} = \begin{pmatrix} \frac{10}{3} \\ \frac{26}{3} \\ \frac{26}{3} \end{pmatrix}, \quad \{b_{ij}\} = \begin{pmatrix} \frac{4447}{6} & \frac{249}{2} & \frac{249}{2} \\ \frac{1245}{2} & \frac{779}{3} & 48 \\ \frac{1245}{2} & 48 & \frac{779}{3} \end{pmatrix}$
G_3	broken at $Q = M_3$
$\downarrow$	$\{b_i\} = \begin{pmatrix} -7 \\ -2 \\ -2 \\ 7 \end{pmatrix}, \quad \{b_{ij}\} = \begin{pmatrix} -26 & \frac{9}{2} & \frac{9}{2} & \frac{1}{2} \\ 12 & 31 & 6 & \frac{27}{2} \\ 12 & 6 & 31 & \frac{27}{2} \\ 4 & \frac{81}{2} & \frac{81}{2} & \frac{115}{2} \end{pmatrix}$
G_2	broken at $Q = M_2$
$\downarrow$	$\{b_i\} = \begin{pmatrix} -7 \\ -\frac{8}{3} \\ -2 \\ \frac{11}{2} \end{pmatrix}, \quad \{b_{ij}\} = \begin{pmatrix} -26 & \frac{9}{2} & \frac{9}{2} & \frac{1}{2} \\ 12 & \frac{37}{3} & 6 & \frac{3}{2} \\ 12 & 6 & 31 & \frac{27}{2} \\ 4 & \frac{9}{2} & \frac{81}{2} & \frac{61}{2} \end{pmatrix}$
G_1	broken at $Q = M_1$
$\downarrow$	$\{b_i\} = \begin{pmatrix} -7 \\ -\frac{19}{6} \\ \frac{41}{10} \end{pmatrix}, \quad \{b_{ij}\} = \begin{pmatrix} -26 & \frac{9}{2} & \frac{11}{10} \\ 12 & \frac{35}{6} & \frac{9}{10} \\ \frac{44}{5} & \frac{17}{10} & \frac{199}{50} \end{pmatrix}$
$G_{\rm SM}$	

Table 5. Coefficients b_i and b_{ij} of gauge coupling β functions appearing in the specified breaking chain.

2. RG evolve the G_1 gauge couplings from the scale M_1 to M_2, where G_2 is recovered, and the gauge couplings of G_2 are obtained via matching conditions at scale M_2.

3. Repeating this same procedure, to evolve all couplings to the GUT scale, M_X, to unify to a single value α_X with the matching condition at M_X fully accounted for.

The above RG running procedure involves four scales M_1, M_2, M_3 and M_X. Gauge unification requires that three SM gauge couplings meet each other at the GUT scale, up to matching conditions, and enforces two constraints; thus, there are only two free scales. The remaining scales and the gauge coupling, α_X, are then determined via gauge unification. General restrictions on the parameter space of scales i.e., M_2, M_3 and M_X varying with M_1, are shown in the left plot of figure 1.

Given the gauge unification scale, M_X, and its gauge coupling at that scale, the proton lifetime via the decaying process $p \to \pi^0 e^+$ is predicted. Due to the scale correlations imposed by gauge unification, the correlation between the proton lifetime, τ_p, and M_X can

JHEP11(2022)072

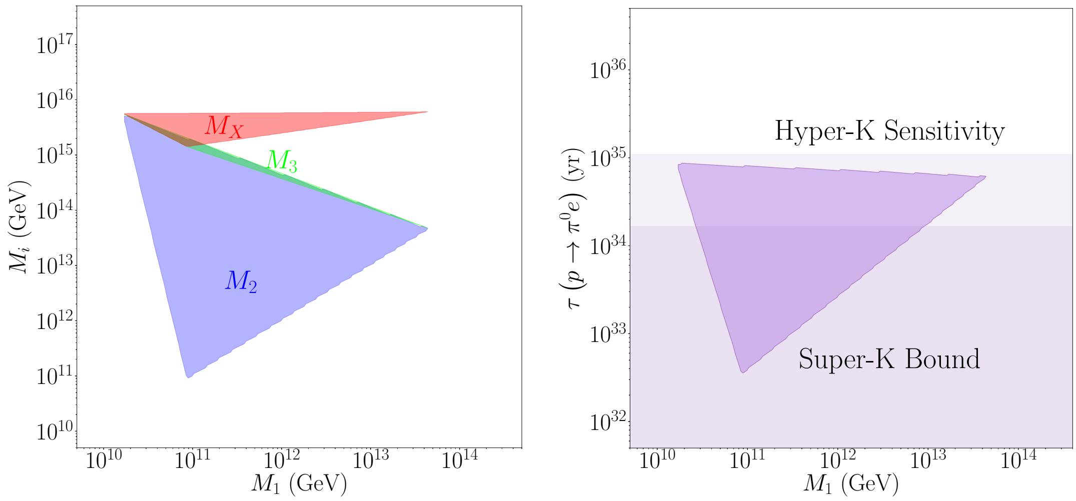

Figure 1. Left panel: regions of M_2, M_3, M_X as functions of M_1 allowed by gauge unification; right panel: prediction of proton lifetime as functions of M_1, with exclusion upper bound of Super-K and future sensitivity of Hyper-K indicated.

be transformed into a correlation between τ_p and any intermediate scale. Following the formulation of ref. [12], we derive the allowed parameter space of τ_p versus intermediate scales. By varying the lowest intermediate scale M_1, we obtain general regions of τ_p. The bound of τ_p versus the lowest scale M_1 is shown in the right panel of figure 1. The Super-K experiment set a lower bound on the proton lifetime, $\tau(p \to e^+\pi^0) > 2.4 \times 10^{34}$ years at 90 % confidence level [13]. In the future, Hyper-Kamiokande (Hyper-K) is expected to improve the measurement of proton lifetime by almost one order of magnitude [20]. If proton decay is not observed, the entire parameter space of this breaking chain will be excluded.

Benchmark Point 1 (BP1). In figure 2, we show an example of the RG running of the gauge couplings along with the scale and fix

$$M_1 = 2 \times 10^{13}\ \text{GeV}\,, \qquad M_2 = 5 \times 10^{13}\ \text{GeV}\,, \tag{2.15}$$

where the remaining scales, M_3 and M_X, as well as the gauge coupling α_X, are then determined via the gauge unification,

$$M_3 = 7.55 \times 10^{13}\ \text{GeV}\,, \qquad M_X = 5.68 \times 10^{15}\ \text{GeV}\,, \qquad \alpha_X = 0.0279\,. \tag{2.16}$$

This benchmark point will be considered throughout this paper. Its associated proton decay rate, $\tau(p \to e^+\pi^0) \sim 5.1 \times 10^{34}$ years, is consistent with the current Super-K bound and will be tested by Hyper-K. We note that BP1 is consistent with SM fermion masses and mixing to a high statistical significance, and this requires $M_1 \sim 10^{13}$ GeV. Such a high value for M_1 leads a compressed hierarchy between M_1, M_2 and M_3 and this comes from the constraint of gauge unification (from the left panel of figure 1 this region is in the right corner of the blue triangle.)

JHEP11(2022)072

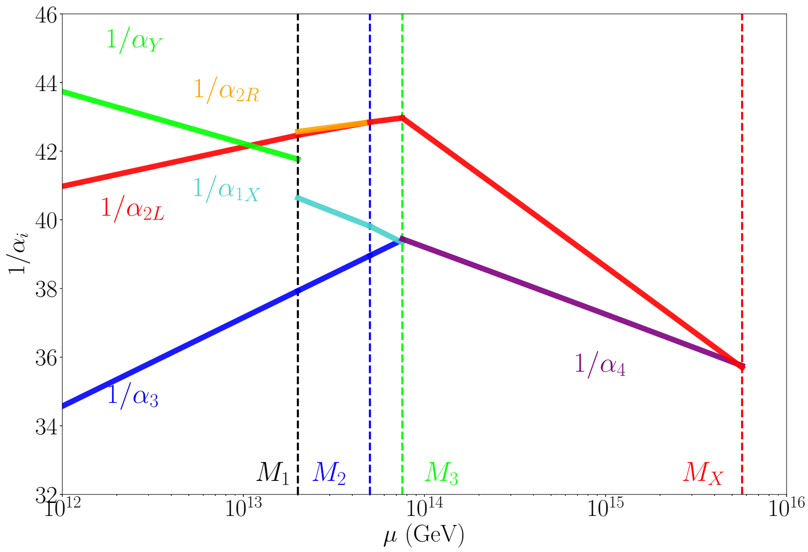

Figure 2. The RG running of gauge couplings in the breaking chain $SO(10) \to G_3 \to G_2 \to G_1 \to G_{SM}$. BP1 with the first and second lowest intermediate scales are fixed at $M_1 = 2 \times 10^{13}$ GeV and $M_2 = 5 \times 10^{13}$ GeV, the remaining scales M_3 and M_X, as well as gauge couplings α_{2R}, are determined by the gauge unification at M_X.

3 Fermion masses and mixing

As all the SM fermions are embedded in the same SO(10) multiplet (**16**), their masses are correlated with each other. Therefore, it is a non-trivial task to find regions of the GUT model parameter space that predict the SM fermion masses and mixing consistent with the precisely measured (particularly in the quark sector) experimental data. This section presents the correlations of masses and mixing between quarks and leptons and predicts heavy neutrino masses using the model we discussed in the previous section. We parametrise the up, down, neutrino, charged lepton Yukawa couplings and right-handed neutrino mass matrix, respectively, as follows [35]:

$$Y_u = h + r_2 f + i\, r_3 h' , \qquad Y_d = r_1(h + f + i\, h') , \qquad Y_\nu = h - 3r_2 f + i\, c_\nu h' ,$$
$$Y_e = r_1(h - 3f + i\, c_e h') , \qquad M_{\nu_R} = f\, \frac{\sqrt{3}\, r_1}{V_{16}} v_S , \tag{3.1}$$

where

$$h = Y_{\mathbf{10}} V_{11} , \quad f = Y_{\overline{\mathbf{126}}} \frac{V_{16}}{\sqrt{3}} \frac{V_{11}^*}{V_{15}} , \quad c_e = \frac{V_{17} - \sqrt{3} V_{18}}{V_{17} + V_{18}/\sqrt{3}} , \quad c_\nu = \frac{V_{13}^* - \sqrt{3} V_{14}^*}{V_{17} + V_{18}/\sqrt{3}} \frac{V_{15}}{V_{11}^*} ,$$
$$r_1 = \frac{V_{15}}{V_{11}^*} , \quad r_2 = \frac{V_{12}^*}{V_{16}} \frac{V_{15}}{V_{11}^*} , \quad r_3 = \frac{V_{13}^* + V_{14}^*/\sqrt{3}}{V_{17} + V_{18}/\sqrt{3}} \frac{V_{15}}{V_{11}^*} , \quad h' = -i\, Y_{\mathbf{120}} \left(V_{17} + V_{18}/\sqrt{3} \right) \frac{V_{11}^*}{V_{15}} , \tag{3.2}$$

and V_{ji} denotes the mixing between the mass and interaction basis of the electroweak Higgs doublets. The light neutrino mass matrix, M_ν, is obtained by

$$M_\nu = m_0 Y_\nu f^{-1} Y_\nu , \tag{3.3}$$

where $m_0 = -\frac{V_{16}}{\sqrt{3}\, r_1} \frac{v_{SM}^2}{v_S}$.

3.1 Parametrisation using Hermitian Yukawa matrices

The most general form of Yukawa couplings and neutrino mass matrix includes many free parameters. A considerable reduction in the number of parameters can be achieved by considering only the Hermitian case for all fermion Yukawa couplings matrices Y_u, Y_d, Y_ν and Y_e (and M_R should be real as a consequence of the Majorana nature for right-handed neutrinos). Such a reduction can result from spontaneous CP violation [36, 37] which assumes that there exists a CP symmetry above the GUT scale, leading to real-valued $Y_{\mathbf{10}}$, $Y_{\overline{\mathbf{126}}}$ and $Y_{\mathbf{120}}$, and the CP is broken by some complex VEVs of Higgs multiplets during GUT or intermediate symmetry breaking. For the particular chain we applied in the last section, one can consider, for example, the parity-odd singlet of $G_2 \equiv \mathrm{SU}(3)_c \times \mathrm{SU}(2)_L \times \mathrm{SU}(2)_R \times \mathrm{U}(1)_X \times Z_2^C$, decomposed from $\mathbf{45}$, gains a purely imaginary VEV. Then, via couplings such as $\mathbf{45} \cdot \mathbf{10} \cdot \mathbf{120}$ (and $\mathbf{45} \cdot \overline{\mathbf{126}} \cdot \mathbf{120}$) which generate purely imaginary off-diagonal mass terms between $h^{u,d}_{\mathbf{10}}$ and $h^{u,d}_{\mathbf{120}}$ (and those between $h^{u,d}_{\overline{\mathbf{126}}}$ and $h^{u,d}_{\mathbf{120}}$) and further purely imaginary mixing entries V_{13}, V_{14} (and V_{17}, V_{18}) are obtained. As a result, h, f and h', as well as all parameters on the right-hand side of eq. (3.1), are real. Since h' is antisymmetric, we arrive at Hermitian Dirac Yukawa coupling matrices Y_u, Y_d, Y_ν and Y_e. This texture has widely been applied in the literature, see e.g., refs. [23, 31, 38]. The resulting fermion mass matrices conserve parity symmetry $L \leftrightarrow R$ [31] and following from the assumption that there is no CP violation in the Higgs sector, apart from that of $\mathbf{120}$, r_1, r_2, r_3, c_e, and c_ν are all real parameters resulting in a real symmetric right-handed neutrino mass matrix, M_{ν_R}. The CP symmetry in the Yukawa coupling is spontaneously broken after the Higgses gain VEVs.

For simplicity, we assume that $r_3 = 0$, which implies that the imaginary part of Y_u vanishes. It is convenient to write the up-type Yukawa in the diagonal basis

$$Y_u = h + r_2 f = \mathrm{diag}\{\eta_u y_u, \eta_c y_c, \eta_t y_t\}\,, \tag{3.4}$$

which can be achieved via a real-orthogonal transformation on the fermion flavours without changing the Hermitian property of Y_d, Y_e, and Y_ν. In the above, $\eta_{u,c,t} = \pm 1$ refer to signs that cannot be determined by the real-orthogonal transformation. While $\eta_t = +1$ can be fixed by making an overall sign rotation for all Yukawa matrices, the remaining signs, η_u and η_c, cannot be fixed and are randomly varied throughout our analysis. In the basis of the diagonal up-quark mass matrix, Y_d is given by

$$Y_d = P_a V_{\mathrm{CKM}}\, \mathrm{diag}\{\eta_d y_d, \eta_s y_s, \eta_b y_b\}\, V_{\mathrm{CKM}}^\dagger P_a^*\,, \tag{3.5}$$

where again $\eta_{d,s,b} = \pm 1$ represent the signs of eigenvalues, and V_{CKM} is the CKM matrix parametrised in the following form

$$V_{\mathrm{CKM}} = \begin{pmatrix} c_{12}c_{13} & s_{12}c_{13} & s_{13}e^{-i\delta_q} \\ -s_{12}c_{23} - c_{12}s_{13}s_{23}e^{i\delta_q} & c_{12}c_{23} - s_{12}s_{13}s_{23}e^{i\delta_q} & c_{13}s_{23} \\ s_{12}s_{23} - c_{12}s_{13}c_{23}e^{i\delta_q} & -c_{12}s_{23} - s_{12}s_{13}c_{23}e^{i\delta_q} & c_{13}c_{23} \end{pmatrix}, \tag{3.6}$$

where $s_{ij} = \sin\theta^q_{ij}$, $c_{ij} = \cos\theta^q_{ij}$ and $P_a = \mathrm{diag}\{e^{ia_1}, e^{ia_2}, 1\}$. The matrices h, f and h' are then expressed in terms of Y_u and Y_d

$$h = -\frac{Y_u}{r_2 - 1} + \frac{r_2 \mathrm{Re}Y_d}{r_1(r_2-1)}\,, \qquad f = \frac{Y_u}{r_2-1} - \frac{\mathrm{Re}Y_d}{r_1(r_2-1)}\,, \qquad h' = i\,\frac{\mathrm{Im}Y_d}{r_1}\,,$$

where Y_ν, Y_e are

$$
\begin{aligned}
Y_\nu &= -\frac{3r_2+1}{r_2-1}Y_u + \frac{4r_2}{r_1(r_2-1)}\mathrm{Re}Y_d + i\frac{c_\nu}{r_1}\mathrm{Im}Y_d\,,\\
Y_e &= -\frac{4r_1}{r_2-1}Y_u + \frac{r_2+3}{r_2-1}\mathrm{Re}Y_d + ic_e\mathrm{Im}Y_d\,.
\end{aligned}
\tag{3.7}
$$

The light neutrino mass matrix can be expressed as

$$
\begin{aligned}
M_\nu = m_0 \Bigg(& \frac{8r_2(r_2+1)}{r_2-1}Y_u - \frac{16r_2^2}{r_1(r_2-1)}\mathrm{Re}Y_d \\
& + \frac{r_2-1}{r_1}\left(r_1Y_u + ic_\nu\mathrm{Im}Y_d\right)\left(r_1Y_u - \mathrm{Re}Y_d\right)^{-1}\left(r_1Y_u - ic_\nu\mathrm{Im}Y_d\right)\Bigg)\,.
\end{aligned}
\tag{3.8}
$$

Using this parametrisation, all six quark masses and four CKM mixing parameters are treated as inputs, and we are then left with seven parameters (a_1, a_2, r_1, r_2, c_e, c_ν, and m_0) to fit eight observables, including three Yukawa couplings y_e, y_μ, y_τ, two neutrino mass-squared differences Δm^2_{21}, Δm^2_{31} and three mixing angles θ_{12}, θ_{13}, θ_{23}, where the leptonic CP-violating phase, δ, will be treated as a prediction.[2]

3.2 Procedure of numerical analysis

This section describes how we identify regions of our model parameter space consistent with fermion masses and mixing while evading the existing proton decay limit. In our numerical analysis, we use the following experimental data:

- We fix the Yukawa couplings (y) of charged fermions and CKM mixing angles (θ) at their best-fit (bf) values [23, 39, 40]

$$
\begin{aligned}
y_u^{\rm bf} &= 2.54\times10^{-6}\,, & y_c^{\rm bf} &= 1.37\times10^{-3}\,, & y_t^{\rm bf} &= 0.43\,,\\
y_d^{\rm bf} &= 6.56\times10^{-6}\,, & y_s^{\rm bf} &= 1.24\times10^{-4}\,, & y_b^{\rm bf} &= 5.7\times10^{-3}\,,\\
y_e^{\rm bf} &= 2.70\times10^{-6}\,, & y_\mu^{\rm bf} &= 5.71\times10^{-4}\,, & y_\tau^{\rm bf} &= 9.7\times10^{-3}\,,
\end{aligned}
\tag{3.9}
$$

  and

$$
\theta_{12}^{q,\rm bf} = 0.227\,,\quad \theta_{23}^{q,\rm bf} = 4.858\times10^{-2}\,,\quad \theta_{13}^{q,\rm bf} = 4.202\times10^{-3}\,,\quad \delta^{q,\rm bf} = 1.207\,.
\tag{3.10}
$$

  These values are obtained by RG evolving the experimental best-fit values at a low scale to 2×10^{16} GeV, where we have ignored the experimental errors. For simplicity, small corrections induced by RG running above intermediate scales have been ignored, but their inclusion would further relax the parameter space.[3] However, as we will later see, fixing them at the best fit values is sufficient to reproduce all mixing data. Thus, in this current discussion, we will ignore them for simplicity.

[2]While we do not show the Majorana phases, we compute the effective Majorana mass.

[3]Although the coupling for the heaviest RH neutrino in eq. (2.6) can be of order 1, its contribution to RG running is under control and is expected to be at most 5% as $M_X/M_1 \sim 10^{-2}$.

JHEP11(2022)072

- In the neutrino sector, we use the best-fit values from NuFIT 5.1 [41] and include the 1σ uncertainty. Those data with and without Super-K atmospheric data are, respectively, given by

$$\begin{aligned} &\Delta m^2_{21} = (7.42 \pm 0.21) \times 10^{-5}\ \mathrm{eV}^2\,, \qquad \Delta m^2_{3l} = (2.510 \pm 0.027) \times 10^{-3}\ \mathrm{eV}^2\,, \\ &\theta_{12} = 33.45^\circ \pm 0.77^\circ\,, \qquad \theta_{23} = 42.1^\circ \pm 1.1^\circ\,, \qquad \theta_{13} = 8.62^\circ \pm 0.12^\circ\,, \end{aligned} \tag{3.11}$$

  and

$$\begin{aligned} &\Delta m^2_{21} = (7.42 \pm 0.21) \times 10^{-5}\ \mathrm{eV}^2\,, \qquad \Delta m^2_{3l} = (2.514 \pm 0.028) \times 10^{-3}\ \mathrm{eV}^2\,, \\ &\theta_{12} = 33.44^\circ \pm 0.77^\circ\,, \qquad \theta_{23} = 49.0^\circ \pm 1.3^\circ\,, \qquad \theta_{13} = 8.57^\circ \pm 0.13^\circ\,. \end{aligned} \tag{3.12}$$

  The atmospheric mixing angle, θ_{23}, is restricted to first octant ($0 < \theta_{23} < 45^\circ$) and the second ($45^\circ < \theta_{23} < 90^\circ$), respectively, in the two cases. In both cases, normal ordering (i.e., $m_1 < m_2 < m_3$) of neutrino masses is assumed. Inverted ordering (i.e., $m_3 < m_1 < m_2$) will not be discussed as a preliminary scan indicates that our model does not favour the inverted ordering. We do not consider the small flavour-dependent RG running effect due to the suppression of charged lepton Yukawa coupling.

The statistical analysis is performed in the following way:

- As quark masses and mixing parameters are fixed at their best-fit values, Y_u is fully determined except for the signs of η_u and η_d (note that $\eta_t = +1$ is fixed by an overall sign rotation). Y_d depends on two free model parameters, a_1 and a_2, and signs (η_d, η_s, η_b).

- Based on eq. (3.7), Y_e depends on the two phases a_1, a_2 and three ratios r_1, r_2, c_e up to the above sign differences. Note that Y_e must satisfy three equations simultaneously:

$$\begin{aligned} \mathrm{Tr}\left[Y_e Y_e^\dagger\right] &= y_e^2 + y_\mu^2 + y_\tau^2\,, \\ \mathrm{Tr}\left[Y_e Y_e^\dagger Y_e Y_e^\dagger\right] &= y_e^4 + y_\mu^4 + y_\tau^4\,, \\ \mathrm{Det}\left[Y_e Y_e^\dagger\right] &= y_e^2 y_\mu^2 y_\tau^2\,, \end{aligned} \tag{3.13}$$

  and as the right hand side is fixed, r_1, r_2 and c_e are fully determined by the phases a_1, a_2 and the signs η_q (for $q = u, c, d, s, b$). We scan the phase parameters in the range $a_1, a_2 \in [0, 2\pi]$ and vary the signs $\eta_q = \pm 1$ randomly and solve for r_1, r_2 and c_e. Then, we substitute these values into eq. (3.7) and determine the unitary matrix V_e used in the diagonalisation $V_e^\dagger Y_e Y_e^\dagger V_e = \mathrm{diag}\{y_e^2, y_\mu^2, y_\tau^2\}$.

- In eq. (3.8), the neutrino mass matrix, M_ν, is determined by two further parameters c_ν and m_0. The former determines the flavour structure and the latter the absolute mass scale, and by scanning these parameters, we determine M_ν. The diagonalisation $V_\nu^\dagger M_\nu V_\nu^* = \mathrm{diag}\{m_1, m_2, m_3\}$ provides the neutrino mass eigenvalues and unitary matrix V_ν.

- The PMNS matrix is given by $U_{\text{PMNS}} = V_e^\dagger V_\nu$, and the three leptonic mixing angles are derived via

$$\sin\theta_{13} = |(U_{\text{PMNS}})_{e3}|\,, \qquad \tan\theta_{12} = \left|\frac{(U_{\text{PMNS}})_{e2}}{(U_{\text{PMNS}})_{e1}}\right|\,, \qquad \tan\theta_{23} = \left|\frac{(U_{\text{PMNS}})_{\mu 3}}{(U_{\text{PMNS}})_{\tau 3}}\right|\,. \tag{3.14}$$

These angles and two mass squared differences $\Delta m^2_{21} = m^2_2 - m^2_1$ and $\Delta m^2_{31} = m^2_3 - m^2_1$ are taken as outputs to compare with the experimental data shown in eq. (3.11).

In summary, once the charged fermion masses and quark mixing parameters are fixed, we are left with only four free model parameters a_1, a_2, c_ν, m_0 and signs η_q:

$$\mathcal{P}_m \in \{a_1, a_2, c_\nu, m_0, \eta_q\}\,. \tag{3.15}$$

We scan the model parameter space, $\mathcal{P}_m$, to fit five observables:

$$\mathcal{O}_n \in \{\theta_{12}, \theta_{13}, \theta_{23}, \Delta m^2_{21}, \Delta m^2_{31}\}\,. \tag{3.16}$$

In this way, we efficiently reduce the dimensionality of the parameter space from 17 to 5 dimensions. Following the above simplified treatment, we scan two phases a_1, a_2 in the range $[0, \pi]$. The coefficient $|c_\nu|$ is logarithmically scanned in the range $[10^{-3}\,, 10^3]$, and we randomly assign its $\pm$ sign. m_0 (meV) is solved by minimising the χ^2 function, which is used as a measure of how well our model fits the data, being defined as

$$\chi^2 = \sum_n \left[\frac{\mathcal{O}_n(\mathcal{P}_m) - \mathcal{O}_n^{\text{bf}}}{\sigma_{\mathcal{O}_n}}\right]^2\,. \tag{3.17}$$

Given the predefined theory model parameter space, $\mathcal{P}_m$, and scanning in the relevant ranges of these parameters, we determine which regions fit the experimental data by setting an upper bound of χ^2 value. This procedure of the scan is divided into two steps: we first perform a preliminary scan by setting the upper bound of $\chi^2 < 100$ and then perform a subsequent scan to find the points with $\chi^2 < 10$. The results of the first scan which uses the neutrino oscillation data of eq. (3.11) (first octant) are shown in figure 3. A two-dimensional subspace of a_1-a_2 (m_0-c_ν) is shown in the top (bottom) left panel and predictions of θ_{23}-δ (M_{N_1}-M_{N_3}) are given in the right top (bottom) panel. M_{N_1}, M_{N_2} and M_{N_3} are three right-handed neutrino masses ordered from lightest to heaviest, and they are obtained by solving the inverse of the Type-I seesaw formula:

$$M_{\nu_R} = Y_\nu^T M_\nu^{-1} Y_\nu v_{\text{SM}}^2\,, \tag{3.18}$$

where the mass states of ν_R, from the lightest to heaviest, are denoted as N_1, N_2 and N_3. We impose an upper bound by requiring $M_{N_3} \lesssim M_1$, and this is approximately equivalent to requiring that the largest eigenvalue of $Y_{\overline{\mathbf{126}}} \lesssim 1$ such that the perturbativity is respected. Since the maximal value of M_1 allowed by proton decay measurements is given by 4.4×10^{13} GeV [12], viable points in the model parameter space require that

$$M_{N_3} < 4.4 \times 10^{13}\ \text{GeV}\,. \tag{3.19}$$

JHEP11(2022)072

Figure 3. Two-dimensional correlations between theory inputs (left two panels) and predicted observables (right two panels) for $\chi^2 < 100$ for $\theta_{23} \leq 45°$. Consistency with gauge unification is not considered.

Naively, by assuming the magnitude of the Dirac Yukawa coupling $Y_\nu \sim \mathcal{O}(1)$, we know from the seesaw formula that the RHN mass scale is around 10^{15} GeV. Thus, one can expect that the condition of eq. (3.19) rules out most points. This is confirmed by the bottom-left panel figure 3 where most of the points predict the heaviest neutrino mass, M_{N_3}, to be heavier than 4.4×10^{13} GeV. Therefore, these points are not consistent with the requirement of gauge unification. We then perform a second more dense scan around the former points by requiring $\chi^2 < 10$ and gauge unification, e.g., the bound of the heaviest right-handed neutrino mass satisfying eq. (3.19). The results of this scan are shown in figures 4 and 5, where neutrino oscillation data in eqs. (3.11) and (3.12) are used, respectively. In both figures, scatter plots of parameters are shown in the left panel and predictions of observables are given in the right panel. In the first 2×2 grid of both figures, we arrange two-dimensional subspaces of a_1-a_2, m_0-c_ν (left), and predictions θ_{23}-δ, M_{N_1}-M_{N_3} (right). We have checked that truncating the upper bound of χ^2 from 100 to 10 removes most of the